



Preparation, characterization and application of *p*-*tert*-butyl-calix[4]arene-SBA-15 mesoporous silica molecular sieves

Huayu Huang^{a,b}, Chuande Zhao^a, Yongsheng Ji^a, Rong Nie^a, Pan Zhou^a, Haixia Zhang^{a,*}

^a State Key Laboratory of Applied Organic Chemistry, Lanzhou University, 730000, China

^b Department of Science, Nanjing Agricultural University, Nanjing 210095, China

ARTICLE INFO

Article history:

Received 7 July 2009

Received in revised form 27 January 2010

Accepted 27 January 2010

Available online 4 February 2010

Keywords:

Mesoporous silica molecular sieves

Calix[4]arene

Phenol

Adsorption

ABSTRACT

p-*tert*-Butyl-calix[4]arene-SBA-15 mesoporous silica molecular sieves have been prepared and characterized by Fourier transform infrared (FT-IR) spectroscopy, powder X-ray diffraction (XRD) and nitrogen adsorption–desorption measurements. FT-IR spectra showed the presence of methylene (–CH₂–), methyl (–CH₃) and phenyl bands on the modified SBA-15. Powder XRD data indicated the structure of *p*-*tert*-butyl-calix[4]arene-SBA-15 remained the host SBA-15 structure. Brunauer–Emmett–Teller (BET) surface area analysis revealed a decrease in surface area and pore size. The adsorption capacity of the materials to diethylstilbestrol and bisphenol A was studied via the dynamic adsorption experiments. The maximum dynamic adsorption capacity on modified materials was 34.8 and 2.9 times higher than SBA-15 particles for diethylstilbestrol and bisphenol A, respectively. The results indicated that *p*-*tert*-butyl-calix[4]arene-SBA-15 particles could be used to enrich the various compounds in water samples before the further analysis.

© 2010 Elsevier B.V. All rights reserved.

1. Introduction

Silica materials with functional groups have been widely used as solid phase in high performance liquid chromatography (HPLC) [1] and solid phase extraction (SPE) [2]. Mesoporous SBA-15 silica molecular sieves with large pore diameter (up to 30 nm) and area (up to 1000 m² g^{−1}) [3], show excellent homogeneity and stability and can be well controlled for adsorption/desorption processes [4]. Recently, mesoporous SBA-15 silica molecular sieves have been modified with 3-mercaptopropyl, 3-aminopropyl, octyltrimethoxy or octadecyltrimethoxy siloxanes [5–8] for the separation and analysis of inorganic ions, organic compounds and biological molecules. Depending on the different chemical groups, the modified materials normally exhibited different properties and had the flexibility to be further modified for a variety of applications.

A calixarene is a macrocycle or cyclic oligomer based on a hydroxyalkylation product of a phenol and an aldehyde, which have been widely used as platforms to build receptors that are able to bind ions and molecules of biological and environmental relevance [9]. Calixarenes and their derivatives could be selected to use in analysis and separation fields because of the size of macrocycle and the properties of substituted chemical groups. We proposed a convenient and effective procedure for the modifi-

cation with *p*-*tert*-butyl-calix[4]arene on the mesoporous SBA-15 silica materials. Usually, chemical groups could be loaded into SBA-15 through the reaction of Si–OH and Si–Cl [4,10,11], or Si–OH and Si–OR [6,8,12]. Chloro silanes could react with water of the air and are more expensive than alkoxy silanes. Furthermore, HCl from the reaction of Si–OH and Si–Cl could be adsorbed by the silica materials and may make Si–C bond-breaking. Alkoxy silanes are less hazardous for environment and human and used very widely for preparation of chromatographic materials [13]. In the work, for the first step of this modification, epoxide group of 3-glycidoxypropyltrimethoxysilane contacted –OH of *p*-*tert*-butyl-calix[4]arene. The second step took place by forming Si–O–Si bonds due to the interaction between Si–OH and Si–OCH₃. Si–O–Si bonds could be formed further between the adjacent Si–OCH₃ groups. Fourier transform infrared (FT-IR) spectroscopy, powder X-ray diffraction (XRD) and surface area analysis were used to characterize the materials.

Phenol and substituted phenols are important pollutants in water due to their widespread use in industrial processes [14]. Diethylstilbestrol (4,4'-(1,2-diethyl-1,2-ethenediyl)bisphenol, DES) and bisphenol A [2,20-bis(4-hydroxyphenyl)propane, BPA] are strong estrogens, which have widespread application in the production. Because of their high toxicity [15,16], it is very important to remove the residual DES and BPA from water samples. Fig. 1 shows the structures of DES and BPA.

The aim of the study was to develop a method for preparing *p*-*tert*-butyl-calix[4]arene-SBA-15 as a sorbent to remove DES and

* Corresponding author. Tel.: +86 931 4165997; fax: +86 931 8912582.
E-mail address: zhanghx@lzu.edu.cn (H. Zhang).

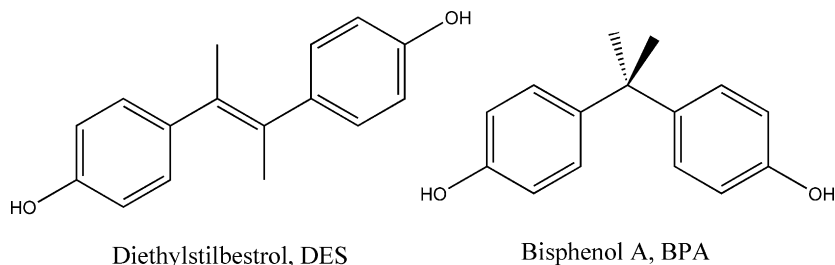


Fig. 1. The structures of diethylstilbestrol (DES) and bisphenol A (BPA).

BPA from aqueous solutions and evaluate the adsorption of DES and BPA on the modified materials by the dynamic adsorption experiments.

2. Materials and experimental

2.1. Materials

Mesoporous SBA-15 silica molecular sieves were purchased from Changchun Jilin University High-Tech. Co. Ltd. (Jilin, China). 3-Glycidoxypropyltrimethoxysilane was purchased from Fluka (Buchs, Switzerland). Formaldehyde, sodium hydroxide, phenyl ether, ethyl acetate, acetic acid, acetone, toluene, dichloromethane, methanol and hydrochloride were purchased from Tianjin Chemical Reagent Co. Ltd. (Tianjin, China). *p*-*tert*-Butylphenol, diethylstilbestrol and bisphenol A were purchased from Sigma (St. Louis, USA). Deionized water was prepared using a Millipore unit (Bedford, MA, USA).

2.2. Materials preparation

2.2.1. Synthesis of *p*-*tert*-butyl-calix[4]arene

The synthesis method of *p*-*tert*-butyl-calix[4]arene was followed as reported previously [17]. A mixture of 20 g of *p*-*tert*-butylphenol, 12 mL of 37% formaldehyde solution and 0.24 g of sodium hydroxide in 0.6 mL of water was placed in a three-necked flask equipped with a mechanical stirrer. The mixture was allowed to stir for 15 min at room temperature and then heated to 110 °C for 2 h. After reaction, the yellow product obtained was dissolved with phenyl ether. The mixture was stirred and heated at 110 °C with a heating mantle while a stream of nitrogen is blown rapidly over the reaction mixture. When a solid started to form, the mixture was stirred and heated to 155 °C for 4 h. The resulting mixture was filtered and washed with ethyl acetate, acetic acid, water and acetone to obtain crude product. The crude product was dissolved in boiling toluene and concentrated. On cooling, white rhombic crystals were obtained. *p*-*tert*-Butyl-calix[4]arene: ¹H NMR (300 MHz, CDCl₃, TMS) δ = 1.21 (36H, s, C(CH₃)₃), 7.01 (8H, s, Ar-H) and 10.3 (4H, s, OH).

2.2.2. Synthesis of *p*-*tert*-butyl-calix[4]arene-SBA-15

SBA-15 was soaked in 0.1 mol L⁻¹ HCl for 24 h, filtered, washed with deionized water and dried in an oven at 100 °C for 8 h.

The synthesis of *p*-*tert*-butyl-calix[4]arene-SBA-15 was carried out following the description of the published literature [18]. 1 mL 3-glycidoxypropyltriethoxysilane and 0.5 g *p*-*tert*-butyl-calix[4]arene were heated under reflux with three drops of perchloric acid as catalyst in 100 mL dry toluene at 80 °C for 15 h in an inert atmosphere of nitrogen gas. The reaction was then cooled and 1 g SBA-15 was added. Also in an inert atmosphere of nitrogen gas the mixture was allowed to react at 110 °C for 48 h. The bonded-material was filtered and washed in sequence with toluene, dichloromethane, water, methanol and acetone. The final

materials were dried in a low pressure oven at 50 °C for 12 h. Fig. 2 shows a flow diagram for preparation of *p*-*tert*-butyl-calix[4]arene-SBA-15.

2.3. Characterization

FT-IR spectra were recorded on a NICOLET 360 FT-IR instrument (Nicolet, USA).

The narrow-angle powder XRD patterns from 0.4° to 10° were collected at D/max-2400 (Rigaku, Japan) instrument using Cu Kα radiation.

Nitrogen adsorption-desorption experiments were carried out at 76.53 K on an ASAP 2010 accelerated surface area and porosimetry system (Micromeritics, USA). The Brunauer-Emmett-Teller (BET) surface area (*S*_{BET}) was calculated from the linearity of the BET equation. The surface area, volume and pore diameter were calculated from the pore size distribution curves using the Barrett-Joyner-Halenda (BJH) formula.

2.4. Adsorption

The adsorption of DES and BPA was measured via the dynamic adsorption experiments on a Ps181-2 wriggle pump (Beijing purkinje general instrument Co. Ltd., China) equipped with TU-1810 UV-vis detector (Beijing purkinje general instrument Co. Ltd., China). 10 μg mL⁻¹ of DES and BPA aqueous solutions were used as mobile phase at a flow-rate of 0.5 mL min⁻¹ and detected at 254 nm for diethylstilbestrol and 278 nm for bisphenol A without column, respectively. When the dynamic adsorption system was equilibrated with the above solution until the UV signal became constant, the column load with SBA-15 or the modified materials was contacted into the dynamic adsorption system. The UV signal changed and then became constant when the column was equilibrated due to adsorption. The interval of time, Δ*t*, was recorded. The adsorption capacity of DES and BPA on the particles, *A*, was calculated following the formula: $A = (C \times v \Delta t) / m$, where *C* is the concentration of compounds in the aqueous solution, *v* is the flow-rate of mobile phase, and *m* is the weight of the material.

3. Results and discussion

3.1. FT-IR

Fig. 3 shows FT-IR spectra of the parent SBA-15, *p*-*tert*-butyl-calix[4]arene and the modified SBA-15 materials. From Fig. 3c, it can be seen that there were methyl (CH₃) asymmetric and symmetric stretching at 2939 and 2887 cm⁻¹, methylene δ_{C-H} at 1450 cm⁻¹, and phenyl ν_{AR}C-C at 1548 cm⁻¹, respectively. The results were closely in agreement with the published data [10,19,20] and indicated that *p*-*tert*-butyl-calix[4]arene was successfully bonded on the surface of the SBA-15 material. The whole band shifts of materials are observed in Table 1 [21,22].

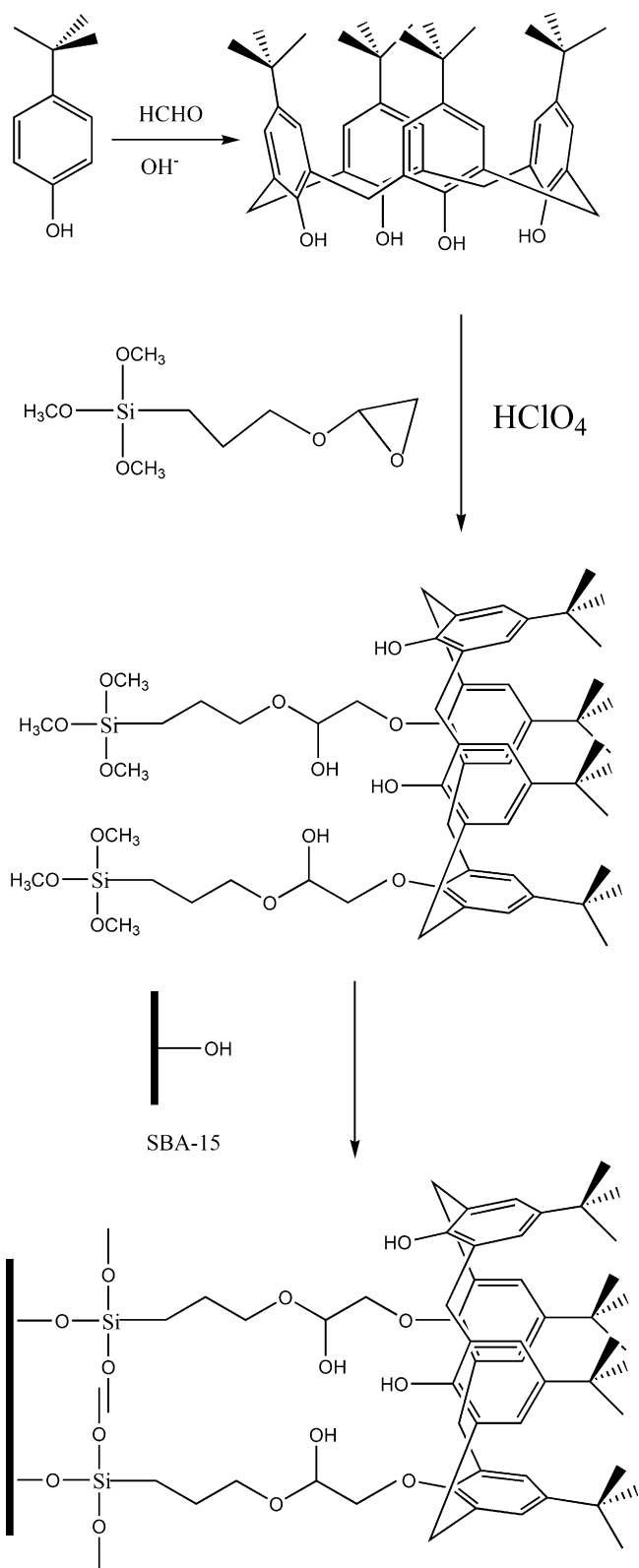


Fig. 2. The route of preparation of *p*-*tert*-butyl-calix[4]arene-SBA-15.

3.2. XRD

XRD patterns of the materials are shown in Fig. 4. In the narrow-angle range peaks for SBA-15 were at 0.8° , 1.4° and 1.7° . For *p*-*tert*-butyl-calix[4]arene-SBA-15, there was one prominent peak at 0.8° and two peaks at 1.5° and 1.7° . These results indicated that

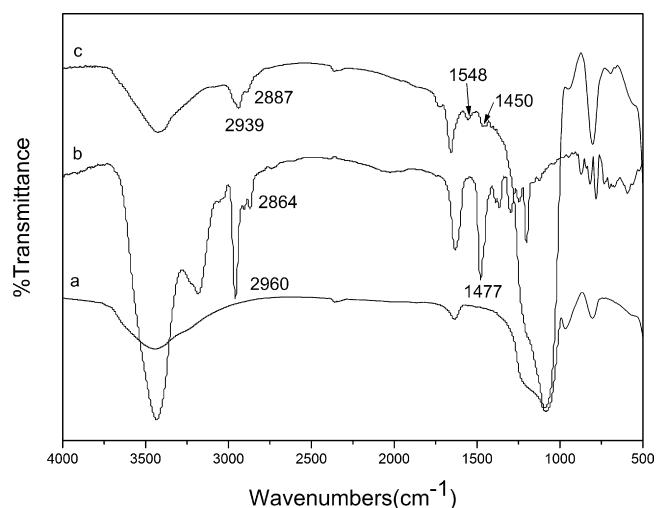


Fig. 3. FT-IR spectra of (a) SBA-15, (b) *p*-*tert*-butyl-calix[4]arene and (c) *p*-*tert*-butyl-calix[4]arene-SBA-15.

p-*tert*-butyl-calix[4]arene-SBA-15 still had a high degree of hexagonal symmetry structure [3,23] and remained the inorganic wall structure of SBA-15 after the modified process.

3.3. Nitrogen adsorption–desorption measurements

Fig. 5 shows nitrogen adsorption–desorption isotherms of the materials, which exhibit a typical IV type isotherm with a H1 hysteresis loop as defined by IUPAC [24]. The H1 hysteresis loop indicated that *p*-*tert*-butyl-calix[4]arene-SBA-15 was still a mesoporous material. However, there was a shift in hysteresis position to low relative pressures and a decreasing trend. The shift of sharp inflection from P/P_0 0.50 to 0.80 is characteristic of a diameter in the mesopore range [12,23]. Pore parameters of materials are shown in Table 2. The BET surface area changed from $524 \text{ m}^2 \text{ g}^{-1}$ to $318 \text{ m}^2 \text{ g}^{-1}$ and the pore diameter decreased from 72.8 \AA to 61.3 \AA on *p*-*tert*-butyl-calix[4]arene-SBA-15. The decrease in surface area and pore diameter indicated that *p*-*tert*-butyl-calix[4]arene group was bonded to the mesoporous channels of SBA-15 successfully [25]. The pore diameter and d_{100} of two materials indicated that the mesopore uniformity of the parent SBA-15 silica was retained in the modified material [11].

3.4. DES and BPA adsorption

The adsorption capacity was one of the important factors to evaluate the mesoporous silica materials as sorbents. The dynamic adsorption experiments were carried out to investigate the adsorption of DES and BPA onto the materials in aqueous solution with the concentration of $10 \mu\text{g mL}^{-1}$ over the range of pH 2.0–10.0. Fig. 6 showed the adsorbed amount of DES and BPA increased on *p*-*tert*-butyl-calix[4]arene-SBA-15 compared to SBA-15. The better results were obtained at pH 7.0, and the adsorption amount on SBA-15 and *p*-*tert*-butyl-calix[4]arene-SBA-15 were 2.04, 71.10 mg g^{-1} for DES, and 5.52, 16.20 mg g^{-1} for BPA, respectively. It was obvious that the maximum dynamic adsorption capacity for DES and BPA was 34.8 and 2.9 times higher than the capacity of SBA-15, respectively. It can be seen that the sample pH value was strongly related to the state of the compounds in the sample solution. BPA (pK_a 9.73 calculated with ACDlab software) and DES (pK_a 10.6) both possess phenolic hydroxyls which present weakly acidic [27]. Under mild conditions, the majority of target compounds were in the molecular state, which facilitated the extraction of compounds. In strongly basic solution, they became anions owing to loss of a pro-

Table 1
Frequencies ν (cm^{-1}) in the FT-IR spectra of SBA-15, *p*-*tert*-butyl-calix[4]arene and *p*-*tert*-butyl-calix[4]arene-SBA-15.

(a) SBA-15		(b) <i>p</i> - <i>tert</i> -Butyl-calix[4]arene		(c) <i>p</i> - <i>tert</i> -Butyl-calix[4]arene-SBA-15	
ν (cm^{-1})	Assignment	ν (cm^{-1})	Assignment	ν (cm^{-1})	Assignment
3445	$\nu(\text{Si-OH})$	3435	$\nu(\text{OH})$	3430	$\nu(\text{Si-OH})$
1633	$\nu(\text{H}_2\text{O})$	2960	$\nu(\text{CH}_3)$	2939	$\nu(\text{CH}_3)$
1078	$\nu(\text{Si-O})$	2905	$\nu(\text{CH}_3)$	2887	$\nu(\text{CH}_3)$
967	$\nu(\text{Si-O})$	2864	$\nu(\text{CH}_3)$	1658	$\nu(\text{H}_2\text{O})$ $\nu(\text{C}_{\text{Ar}}-\text{C}_{\text{Ar}})$
795	$\nu(\text{Si-O})$	1628	$\nu(\text{C}_{\text{Ar}}-\text{C}_{\text{Ar}})$	1548	$\nu(\text{C}_{\text{Ar}}-\text{C}_{\text{Ar}})$
		1477	$\delta(\text{CH}_2)$	1450	$\delta(\text{CH}_2)$
		1366	$\nu(\text{C}_{\text{Ar}}-\text{C}_{\text{Ar}})$	1088	$\nu(\text{Si-O})$
		1290	$\nu(\text{C}_{\text{Ar}}-\text{O})$ $\nu(\text{C}_{\text{Ar}}-\text{C}_{\text{Ar}})$	801	$\nu(\text{Si-O})$
		1250	$\nu(\text{C}-\text{C})$		
		1199	$\nu(\text{C}-\text{C})$		
		871	$\nu(\text{C}-\text{C})$ $\nu(\text{C}_{\text{Ar}}-\text{C}_{\text{Ar}})$		
		821	$\nu(\text{C}-\text{C})$ $\nu(\text{C}_{\text{Ar}}-\text{O})$		
		775	$\delta(\text{C}_{\text{Ar}}\text{C}-\text{C})$		
		740	$\chi(\text{C}_{\text{Ar}}-\text{C}_{\text{Ar}})$		
		705	$\chi(\text{C}_{\text{Ar}}-\text{C}_{\text{Ar}})$		
		594	$\chi(\text{C}_{\text{Ar}}-\text{C}_{\text{Ar}})$		

Table 2
Pore structure parameters of SBA-15 and *p*-*tert*-butyl-calix[4]arene-SBA-15.

Sample	$d(100)^a$ (Å)	S_{BET} ($\text{m}^2 \text{g}^{-1}$)	S_{BJH} ($\text{m}^2 \text{g}^{-1}$)	V_{BJH} ($\text{cm}^3 \text{g}^{-1}$)	D_{BJH} (Å)
SBA-15	95.6	524	546	0.99	72.8
<i>p</i> - <i>tert</i> -Butyl-calix[4]arene -SBA-15	85.2	318	352	10.54	61.3

^a Large unit cell parameter (a_0) = $2d(100)/\sqrt{3}$ [26].

ton. Possessing two active phenolic hydroxyls, BPA and DES tended to protonize in strong acidic solution.

The above results suggested that after the modification of SBA-15 with *p*-*tert*-butyl-calix[4]arene, the larger adsorption of DES occurred, while the adsorption of BPA was relatively weak. We noted that *p*-*tert*-butyl-calix[4]arene, DES and BPA possess a hydroxyl which can act as proton donor as well as proton acceptor in the weak intermolecular interaction. It enlightened us that the different adsorptions of DES and BPA might have something to do with the possible formation of the weak intermolecular interaction between DES (or BPA) and *p*-*tert*-butyl-calix[4]arene. In general, the stronger the interaction is, the larger the adsorption is. Therefore, the larger adsorption of DES may be due to the stronger interaction between DES and *p*-*tert*-butyl-calix[4]arene. We rationalized this possible conclusion in the following section. An important implication of the formation of the weak intermolecular interaction can be seen from FT-IR spectroscopy analysis (Fig. 7). It can be observed that after the adsorptions of DES and BPA, the stretching vibrational frequencies of their hydroxyl groups were shifted to higher values (from 3421 to 3431 cm^{-1} for DES and from 3351 to 3431 cm^{-1} for BPA), which meant that they were blue-shifted. It indicated that the complex between DES (or BPA) and *p*-*tert*-butyl-calix[4]arene might form or exist as weak hydrogen-bonding or van der Waals interactions.

In order to give evidence to the stronger interaction between DES and *p*-*tert*-butyl-calix[4]arene, the theoretical calculations were performed by using hyperchem 7.0 [28] and Gaussian 98

Table 3
Calculated parameters of *p*-*tert*-butyl-calix[4]arene, DES and BPA.

	<i>p</i> - <i>tert</i> -Butyl-calix[4]arene	DES	BPA
$ClgP$	13.384	3.898	3.673
HOMO (a.u.)	-0.19086	-0.19837	-0.20570
LUMO (a.u.)	-0.01451	-0.00641	-0.00274

[29] programs. We used $ClgP$ obtained from the calculation by hyperchem to represent the hydrophobicity of a compound. As summarized in Table 3, the hydrophobicity was in the order: *p*-*tert*-butyl-calix[4]arene > DES > BPA. According to the theory of similarity and intermiscibility, SBA-15 modified by *p*-*tert*-butyl-calix[4]arene may have a larger adsorption for DES than that for BPA. It was in good agreement with the experimental results. The geometries of *p*-*tert*-butyl-calix[4]arene, DES and BPA were optimized at the B3LYP/6-31G(d, p) level of theory. The energies of their highest occupied molecular orbitals (HOMO) and lowest unoccupied molecular orbitals (LUMO) were obtained. Generally, in the two interacting molecules, the closer the value between a molecule's HOMO and the other's LUMO is, the stronger the interaction is [30–32]. As can be seen from Table 3, when the HOMO was located at *p*-*tert*-butyl-calix[4]arene in the intermolecular interaction, it was closer to the LUMO of DES than the LUMO of BPA; on the other hand, when the LUMO was located at *p*-*tert*-butyl-calix[4]arene, it had the smaller gap with the HOMO of DES. It suggested that under any condition, the interaction between *p*-*tert*-

Table 4
Comparison adsorption of DES and BPA on other materials.

Materials	Adsorption concentration ($\mu\text{g mL}^{-1}$)	Adsorption capacity (mg g^{-1})	References
DES	<i>p</i> - <i>tert</i> -Butyl-calix[4]arene-SBA-15	10	71.1
	3-aminopropyl-silicane	40	19.7
	Molecularly imprinted polymer (MIP), (acrylamide as monomer)	24	19.3
BPA	<i>p</i> - <i>tert</i> -Butyl-calix[4]arene-SBA-15	10	16.2
	Hydrophobic zeolite	10	19.0
	β -Cyclodextrin derivative	45.6	84.0

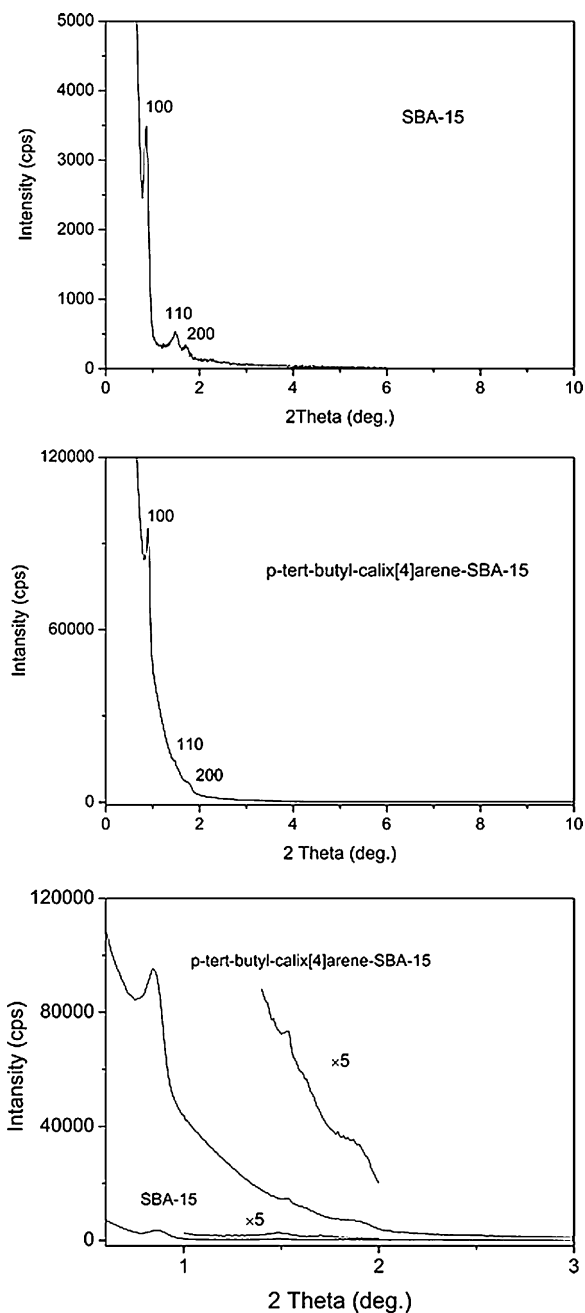


Fig. 4. Powder XRD of SBA-15 and *p*-tert-butyl-calix[4]arene-SBA-15.

butyl-calix[4]arene and DES should be stronger. Therefore, there was a larger adsorption amount of DES on modified materials.

Table 4 shows the comparison between *p*-tert-butyl-calix[4]arene-SBA-15 and other kinds of materials for the adsorption of DES and BPA on adsorption materials. It is obvious that the adsorption capacity for DES on *p*-tert-butyl-calix[4]arene-SBA-15 was higher than the capacity of the reported literatures [33,34]. For BPA, the adsorption capacity was close to the reported result, when the concentration of adsorption solution was similar [35]. If the concentration of adsorption solution increased, the adsorption capacity could also increase [35,36]. *p*-tert-butyl-calix[4]arene-SBA-15 had better adsorption ability due to its mesoporous structure, calixarene structure, higher surface area and interaction of calixarene and phenol.

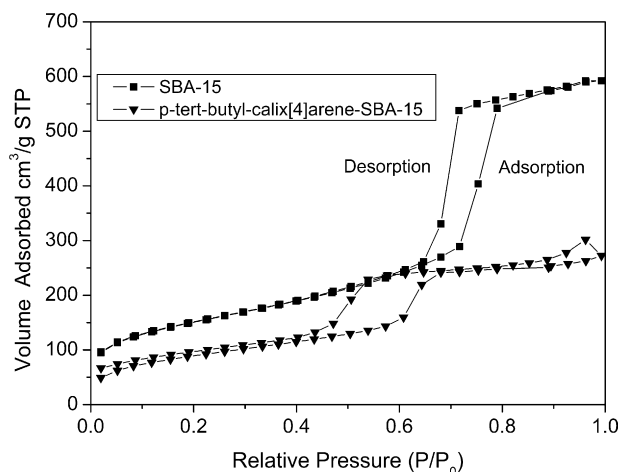


Fig. 5. Nitrogen adsorption-desorption isotherms of SBA-15 and *p*-tert-butyl-calix[4]arene-SBA-15.

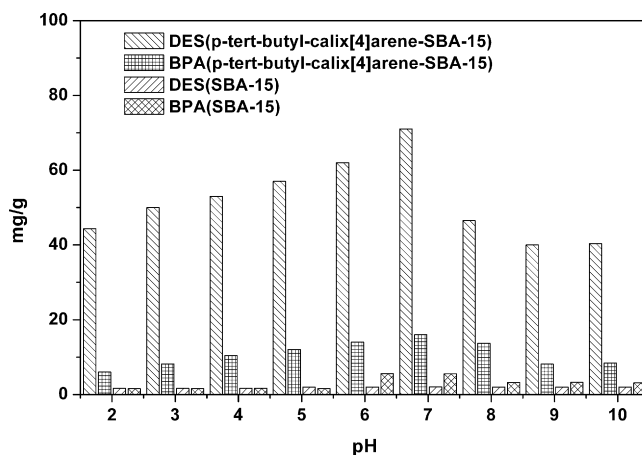


Fig. 6. DES and BPA adsorption on SBA-15 and *p*-tert-butyl-calix[4]arene-SBA-15 over the range of pH 2.0–10.0.

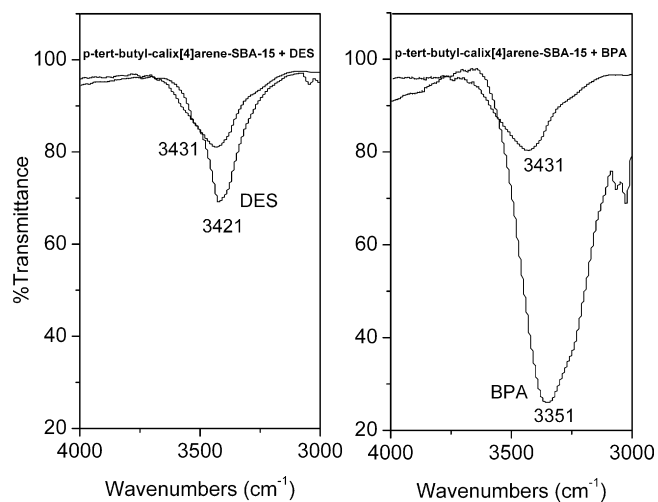


Fig. 7. FT-IR spectra of DES, DES/*p*-tert-butyl-calix[4]arene-SBA-15, BPA and BPA/*p*-tert-butyl-calix[4]arene-SBA-15.

4. Conclusion

The modification of SBA-15 with *p*-*tert*-butyl-calix[4]arene groups was proved successfully and kept the mesoporous structure of the molecular sieves. The modified SBA-15 particles could be used for enrichment of DES and BPA in water samples. Mesoporous SBA-15 silica materials may have further application potential, such as in sensing materials, solid supports and nano-bioelectronics, especially as sorbents that allow the reuse of adsorbent materials for several cycles.

Acknowledgments

This work was supported by the National Natural Science Foundation of China (No. 20775029), the Program for New Century Excellent Talents in University (NCET-07-0400) and the Central Teacher Plan of Lanzhou University.

References

- [1] I. Ferrer, D. Barceló, Validation of new solid-phase extraction materials for the selective enrichment of organic contaminants from environmental samples, *TrAC, Trends Anal. Chem.* 18 (1999) 180–192.
- [2] M.C. Hennion, Solid-phase extraction: method development, sorbents, and coupling with liquid chromatography, *J. Chromatogr. A* 856 (1999) 3–54.
- [3] D.Y. Zhao, J.L. Feng, Q.S. Huo, N. Melosh, G.H. Fredrickson, B.F. Chmelka, G.D. Stucky, Triblock copolymer syntheses of mesoporous silica with periodic 50 to 300 angstrom pores, *Science* 279 (1998) 548–549.
- [4] J.W. Zhao, F. Gao, Y.L. Fu, W. Jin, P.Y. Yang, D.Y. Zhao, Biomolecule separation using large pore mesoporous SBA-15 as a substrate in high performance liquid chromatography, *Chem. Commun.* 7 (2002) 752–753.
- [5] X. Feng, G.E. Fryxell, L.Q. Wang, A.Y. Kim, J. Liu, K.M. Kemner, Functionalized monolayers on ordered mesoporous supports, *Science* 276 (1997) 923–926.
- [6] A.M. Liu, K. Hidayat, S. Kawi, D.Y. Zhao, A new class of hybrid mesoporous materials with functionalized organic monolayers for selective adsorption of heavy metal ions, *Chem. Commun.* 2000 (2000) 1145–1146.
- [7] L. Mercier, T.J. Pinnavaia, A functionalized porous clay heterostructure for heavy metal ion (Hg^{2+}) trapping, *Micropor. Mesopor. Mater.* 20 (1998) 101–106.
- [8] H. Huang, C. Yang, H. Zhang, M. Liu, Preparation and characterization of octyl and octadecyl-modified mesoporous SBA-15 silica molecular sieves for adsorption of dimethyl phthalate and diethyl phthalate, *Micropor. Mesopor. Mater.* 111 (2008) 254–259.
- [9] C. Sgarlata, V. Zito, G. Arena, G.M.L. Consoli, E. Galante, C. Geraci, A sinapic acid-calix[4]arene hybrid selectively binds Pb^{2+} over Hg^{2+} and Cd^{2+} , *Polyhedron* 28 (2009) 343–348.
- [10] R.J. Tian, J.M. Sun, H. Zhang, M.L. Ye, C.H. Xie, J. Dong, J.W. Hu, D. Ma, X.H. Bao, H.F. Zou, Large-pore mesoporous SBA-15 silica particles with submicrometer size as stationary phases for high-speed CEC separation, *Electrophoresis* 27 (2006) 742–748.
- [11] S.A. Mirji, Adsorption of octadecyltrichlorosilane on $\text{Si}(1\ 0\ 0)/\text{SiO}_2$ and SBA-15, *Colloid Surf. A* 289 (2006) 133–140.
- [12] Z.H. Luan, J.A. Fournier, J.B. Wooten, D.E. Miser, Preparation and characterization of (3-aminopropyl)triethoxysilane-modified mesoporous SBA-15 silica molecular sieves, *Micropor. Mesopor. Mater.* 83 (2005) 150–158.
- [13] G.Q. Liu, Z.L. Yu, *Technology of Chromatographic Column*, Chemical Industry Press, Beijing, 2001, p. 163.
- [14] X. Liu, Y. Ji, Y. Zhang, H. Zhang, M. Liu, Oxidized multiwalled carbon nanotubes as a novel solid-phase microextraction fiber for determination of phenols in aqueous samples, *J. Chromatogr. A* 1165 (2007) 10–17.
- [15] R.M. Giusti, K. Iwamoto, E.E. Hatch, Diethylstilbestrol revisited: a review of the long-term health effects, *Ann. Int. Med.* 122 (1995) 778–788.
- [16] F. Cao, P. Bai, H. Li, Y. Ma, X. Deng, C. Zhao, Preparation of polyethersulfone-organophilic montmorillonite hybrid particles for the removal of bisphenol A, *J. Hazard. Mater.* 162 (2009) 791–798.
- [17] C.D. Gutsche, M. Iqbal, *p*-*tert*-butylcalix[4]arene, *Org. Synth.* 8 (1993) 75–78.
- [18] W. Xu, J.S. Li, Y.Q. Feng, S.L. Da, Y.Y. Chen, X.Z. Xiao, Preparation and characterization of *p*-*tert*-butyl-calix[6]arene-bonded silica gel stationary phase for high-performance liquid chromatography, *Chromatographia* 48 (1998) 245–250.
- [19] H. Hoffmann, U. Mayer, A. Krischanitz, Structure of alkylsiloxane monolayers on silicon surfaces investigated by external reflection infrared spectroscopy, *Langmuir* 11 (1995) 1304–1312.
- [20] Z.P. Zhao, X.Y. Zhou, W.M. Zhang, W.K. Zhao, *Instrumental Analysis*, High Education Press, Beijing, 1990, p. 88.
- [21] V.L. Furer, E.I. Borisoglebskaya, V.V. Zverev, V.I. Kovalenko, DFT and IR spectroscopic analysis of *p*-*tert*-butylthiacalix[4]arene, *Spectrochim. Acta Part A* 63 (2006) 207–212.
- [22] C. Shen, J. Wang, Z. Tang, H. Wang, H. Lian, J. Zhang, C. Cao, Physicochemical properties of poly(ethylene oxide)-based composite polymer electrolytes with a silane-modified mesoporous silica SBA-15, *Electrochim. Acta* 54 (2009) 3490–3494.
- [23] A. Sayari, B.H. Han, Y. Yang, Simple synthesis route to monodispersed SBA-15 silica rods, *J. Am. Chem. Soc.* 126 (2004) 14348–14349.
- [24] K.S.W. Sing, D.H. Everett, R.A.W. Haul, L. Moscou, R.A. Pierotti, J. Rouquerol, T. Siemieniewska, Multilayer adsorption of nitrogen and alkanes by non-porous carbons and silicas, *Pure Appl. Chem.* 57 (1984) 603–618.
- [25] S.A. Mirji, S.B. Halligudi, D.P. Sawant, N.E. Jacob, K.R. Patil, A.B. Gaikwad, S.D. Pradhan, Adsorption of octadecyltrichlorosilane on mesoporous SBA-15, *Appl. Surf. Sci.* 252 (12) (2006) 4097–4103.
- [26] L. Vradman, L. Titelman, M. Herskowitz, Size effect on SBA-15 microporosity, *Micropor. Mesopor. Mater.* 93 (2006) 313–317.
- [27] Y. Ji, X. Liu, M. Guan, C. Zhao, H. Huang, H. Zhang, C. Wang, Preparation of functionalized magnetic nanoparticulate sorbents for rapid extraction of biphenolic pollutants from environmental samples, *J. Sep. Sci.* 32 (2009) 2139–2145.
- [28] HyperChem, ver. 7.0, Hypercube, Inc., Gainesville, FL, 2002.
- [29] M.J. Frisch, G.W. Trucks, H.B. Schlegel, G.E. Scuseria, M.A. Robb, J.R. Cheeseman, V.G. Zakrzewski, J.A. Montgomery, R.E. Stratmann, J.C. Burant, S. Dapprich, J.M. Millam, A.D. Daniels, K.N. Kudin, M.C. Strain, O. Farkas, J. Tomasi, V. Barone, M. Cossi, R. Cammi, B. Mennucci, C. Pomelli, C. Adamo, S. Clifford, J. Ochterski, G.A. Petersson, P.Y. Ayala, Q. Cui, K. Morokuma, D.K. Malick, A.D. Rabuck, K. Raghavachari, J.B. Foresman, J. Cioslowski, J.V. Ortiz, B.B. Stefanov, G. Liu, A. Liashenko, P. Piskorz, I. Komaromi, R. Gomperts, R.L. Martin, D.J. Fox, T. Keith, M.A. Al-Laham, C.Y. Peng, A. Nanayakkara, C. Gonzalez, M. Challacombe, P.M.W. Gill, B.G. Johnson, W. Chen, M.W. Wong, J.L. Andres, M. Head-Gordon, E.S. Replogle, J.A. Pople, Gaussian 98, revision A, Gaussian, Inc., Pittsburgh, PA, 1998.
- [30] F.Z. Ren, Y.X. Wang, G.B. Zhang, S.K. Wei, Y.H. Luo, An *ab initio* study of niobium ($n=2-11$) clusters: structure, stability and magnetism, *Chin. Phys. B* 18 (2009) 1491–1497.
- [31] M.T. Baumgartner, R.A. Taccone, M.A. Teruela, S.I. Lane, Theoretical study of the relative reactivity of chloroethenes with atmospheric oxidants (OH , NO_3 , $\text{O}(^3\text{P})$, $\text{Cl}(^2\text{P})$ and $\text{Br}(^2\text{P})$), *Phys. Chem. Chem. Phys.* 4 (2002) 1028–1032.
- [32] B.S. Jursic, Z. Zdravkovski, *Ab initio* study of the 1,3-cycloaddition of ethyl azide to fluorinated acetonitriles, *J. Mol. Struct. (Theochem.)* 333 (1995) 209–214.
- [33] Z. Xu, S. Chen, W. Huang, G. Fang, H. Pingzhu, S. Wang, Study on an on-line molecularly imprinted solid-phase extraction coupled to high-performance liquid chromatography for separation and determination of trace estrone in environment, *Anal. Bioanal. Chem.* 393 (2009) 1273–1279.
- [34] Z. Meng, W. Chen, A. Mulchandani, Removal of estrogenic pollutants from contaminated water using molecularly imprinted polymers, *Environ. Sci. Technol.* 39 (2005) 8958–8962.
- [35] W.-T. Tsai, H.-C. Hsu, T.-Y. Su, K.-Y. Lin, C.-M. Lin, Adsorption characteristics of bisphenol-A in aqueous solutions onto hydrophobic zeolite, *J. Colloid Interf. Sci.* 299 (2006) 513–519.
- [36] M. Kitaoka, K. Hayashi, Adsorption of bisphenol A by cross-linked β -cyclodextrin polymer, *J. Incl. Phenom. Macro. Chem.* 44 (2002) 429–431.